Experimental demonstration of waveguiding in honeycomb and square-lattice silicon photonic crystal membranes

Daniel Puerto[a*], Amadeu Griol[a], José Maria Escalante[a], Bahram Djafari-Rouhani[b], Yan Pennec[b], Vincent Laude[c], Jean-Charles Beugnot[c], and Alejandro Martínez[a]

a. Nanophotonics Technology Center, Universitat Politècnica de València, Valencia, Spain
b. Institut d'Electronique, de Microélectronique et de Nanotechnologie, CNRS UMR 8520, Lille, France
c. Institut FEMTO-ST, Université de Franche-Comté, CNRS UMR 6174, Besançon, France

ABSTRACT

Sub-micron waveguides and cavities have been shown to produce the confinement of elastic and optical waves in the same devices in order to benefit from their interaction. It has been shown that square and honeycomb lattices are the most suitable to produce simultaneous photonic and phononic band gaps on suspended silicon slabs. The introduction of line defects on such "phoxonic" (or optomechanical) crystals should lead to an enhanced interaction between confined light and sound. In this work we report on the experimental measurements of light guiding through waveguides created in these kinds of two-dimensional photonic crystal membranes. The dimensions of the fabricated structures are chosen to provide a "phoxonic" bandgap with a photonic gap around 1550 nm. For both kinds of lattice, we observe a high-transmission band when introducing a linear defect, although it is observed for TM polarization in the honeycomb lattice and for TE in the square. Using the plane-wave expansion and the finite element methods we demonstrate that the guided modes are below the light line and, therefore, without additional losses beside fabrication imperfections. Our results lead us to conclude that waveguides implemented in honeycomb and square lattice "phoxonic" crystals are a very suitable platform to observe an enhanced interaction between propagating photons and phonons.

Keywords: Photonic crystal membranes, phonon, silicon-on-insulator, optomechanics, acousto-optical interactions

1. INTRODUCTION

Photonic crystal slabs (PCSs) are structures with of a periodic lattice of holes in a high-index semiconductor film. This forms a periodic refractive index modulation so that light confinement in the film is achieved by means of total internal reflection and the periodicity permits to create bandgaps to forbid guided-light propagation at certain wavelengths. The introduction of line defects in such PCS is a powerful way to create light waveguides at the nanoscale with some special properties such as lossless propagation through sharp bends [1] or slow-light propagation [2]. The triangular lattice has become extremely popular because it provides a very wide band for even-parity modes (which can be excited using TE polarized light) in PCSs [3]. However, other kinds of lattice display other features that can be of interest for the creation of PCS-based circuits. Specifically, square and honeycomb lattice suspended PCSs have been shown to possess bandgaps not only for photons but also for acoustic waves (phonons) [4,5]. If such PCSs are designed to present bandgaps for guided photons at optical communication wavelengths around 1550 nm, bandgaps for phonons appear for frequencies of some GHz [6]. It is worth mentioning that the frequencies for photonic and phononic gaps are different since the wavelengths that correspond to the band gaps need to be of the same order as the lattice constant. The frequencies of the electromagnetic and elastic gaps do not need to overlap because the gaps relate to waves with different speeds. It has to be stressed that the simultaneous confinement and enhanced interaction of photons and phonons in periodic nanostructures has become a hot-topic in recent years giving rise to the field known as optomechanics [7,8]. If structures such as slow waveguides or cavities for simultaneous spatial and temporal confinement of both photon and phonon waves are realized, their interaction can be extremely enhanced, which would result in a enormous increase of the efficiency of some processes (such as stimulated Brillouin scattering) as well as in novel, dual applications (such as phoxonic sensors). Therefore, it becomes clear that honeycomb- and square-lattice PCSs can become an important platform for optomechanics as well as for demonstration of other acousto-optical effects [9]. In this work, we

demonstrate for the first time to the best of our knowledge the guiding of light in the 1550 nm wavelength region along photonic waveguides created by introducing line defects in honeycomb and square-lattice PCSs built on suspended-silicon slabs.

2. METHODOLOGY

2.1 Fabrication process

The fabrication of the membrane PCS waveguides was carried out by means of an optimized electron beam lithography process depicted in Figure 1. The first step consists of a coating process of 170 nm of PMMA-950k (Poly-methyl methacrylate) positive resist (two spinning processes were carried out to obtain the required resist thickness to ensure a right silicon etching). The PMMA resist is directly exposed by means of a Raith150 electron beam system. This exposure was performed at 10 KeV with and aperture of 30 microns and a write field of 100 microns. Potential proximity effects were corrected by adjusting dose for each element taking into account its placement. In addition, hole radii were also adjusted in the GDS file depending also on the placement of the hole in the structure.

After developing the exposed pattern is transferred into the resist. The resist developing consists of a double paddle process by using commercial MIBK/IPA (Methyl Isobutyl Ketone/ Isopropyl Alcohol) compound as developer and IPA as stopper. It should take into account that exposed areas must be the trenches because as mentioned PMMA positive resist is used to create the etching mask.

The next step consisted on a RIE (Reactive Ion Etching) process based on an ICP (Inductively Coupled Plasma) system was employed to carry out the silicon etching.

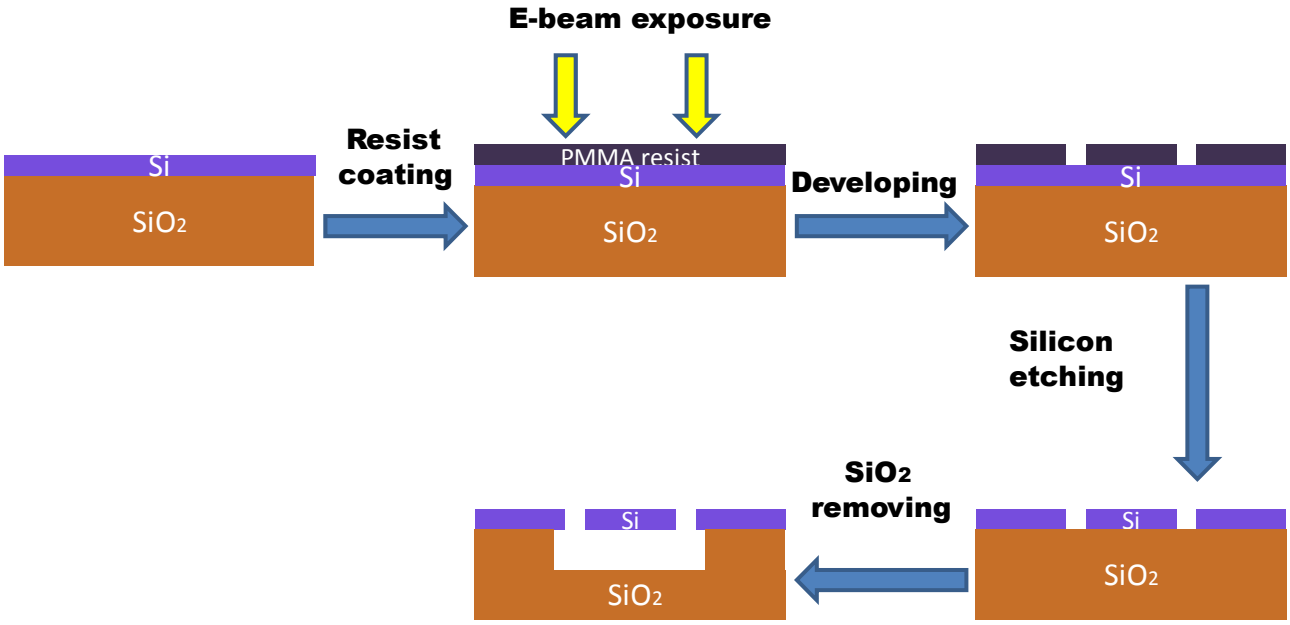

Fig. 1. Scheme of the process developed to fabricate silicon photonic crystal membranes

Finally and in order to release the membranes by locally removing the silica low-cladding a new exposure procedure was used. In this case, and due to the low resolution required, a mask aligner device was employed to open micron size windows on an AZECI-3027 photo resist mask. The last step consisted on a chemical HF (hydro fluidic acid) bath to remove the silica down-cladding and release the membranes.

Using the abovementioned fabrication process we have fabricated phoXonic crystals membranes whit different patterns. Figure 2 shows a two SEM (Scanning Electron Microscope) picture of kind phoXonic crystal devices based on a square and honeycomb lattice. In order to facilitate the measure of the optical properties of these devices we include input and output waveguide (see Fig. 2). The lattice of the square membranes can be fabricated with 0º or 45º degree, whereas the

honeycomb lattice can be orientated with 0º or 90º degree.

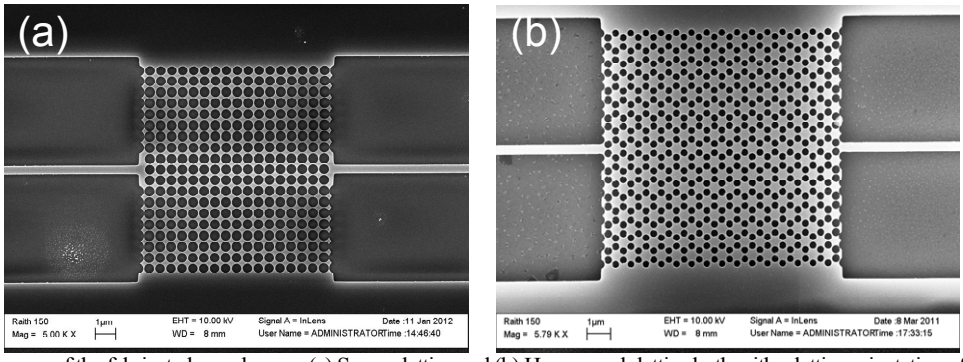

Fig. 2: SEM images of the fabricated membranes: (a) Square lattice and (b) Honeycomb lattice both with a lattice orientation of 0 º degrees.

2.2 Experimental Setup

The experimental setup (Figure 3) used in the optical characterization is formed by a NIR Camera (Alpha sensitive range 900-1680 nm), an optical power meter (Ando AQ2743), a tunable laser (Santec TSL-210F Full-band tunable laser 1260-1630 nm), a linear polarizer (Thorlabs IR Linear Film Polarizers), a lensed fiber, an objective lens (Newport F-L20B) and two XYZ sub-micrometer translation stages (Thorlabs XYZ MAX312). Light from a tunable laser source is coupled into the sample (via 3-μm-width waveguides) using a lensed fiber, whereas the output light is collected by an objective onto a power detector. The two translation stages are used to align the lensed fiber with the PCS input waveguide and the objective lens with the PCS output. The optical power meter detects the transmission signal of the PCS circuit in the full wavelength range (1260-1630 nm), whereas the NIR camera is used to facilitate the alignment process. All the fabricated samples included a suspended 400-nm-width straight photonic waveguide. The response of this waveguide is used as a reference to normalize the transmission measurements of the others circuits.

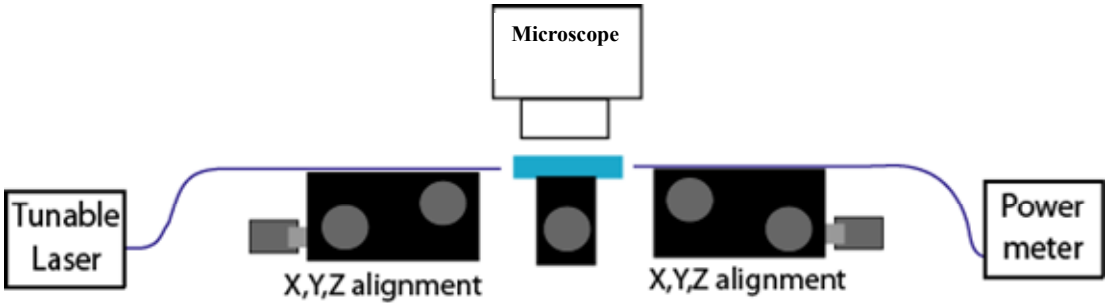

Fig. 3: Sketch of the experimental setup.

3. EXPERIMENTAL AND THEORETICAL RESULTS

3.1 Honeycomb Lattice

Honeycomb-lattice PCSs can be designed to display a complete photonic bandgap in the sense of forbidding guided modes for both odd and even symmetries [4]. However, this complete band gap turns to be quite narrow, which can be very limiting for some applications. From this point of view, it would be more useful to have a wider band gap for a given symmetry, since in PCS-based devices we can separately excite even or odd modes by properly selecting the polarization of the input light. In other words, a photonic band gap occurring for a unique symmetry (odd or even) should be enough for most usual functionalities, such as cavities, waveguides or splitters. Figure 4(a) shows the sketch of a suspended silicon PCS with a honeycomb lattice of holes. In this sketch *a* is the lattice period, *h* is the slab thickness, *r* is the radius of the holes and *d* is the thickness of the photonic waveguide created by introducing a line-defect along the ΓX direction in the otherwise periodic lattice. The parameters (a = 650 nm, r = 160 nm and h = 390 nm) were chosen so that the structure provides a wide photonic band gap for odd-parity modes in the wavelength region around 1550 nm whilst ensuring that it can be fabricated. For instance, a minimum spacing between adjacent holes of 50 nm is considered. Figure 4(b-e) shows SEM images of the released regions in the fabricated sample with a total length of 10 μm and

different d parameter. Whereas, the Figure 4(f-i) shows SEM images of the membranes fabricated with the same d parameter (d=1.6A) but with different total length.

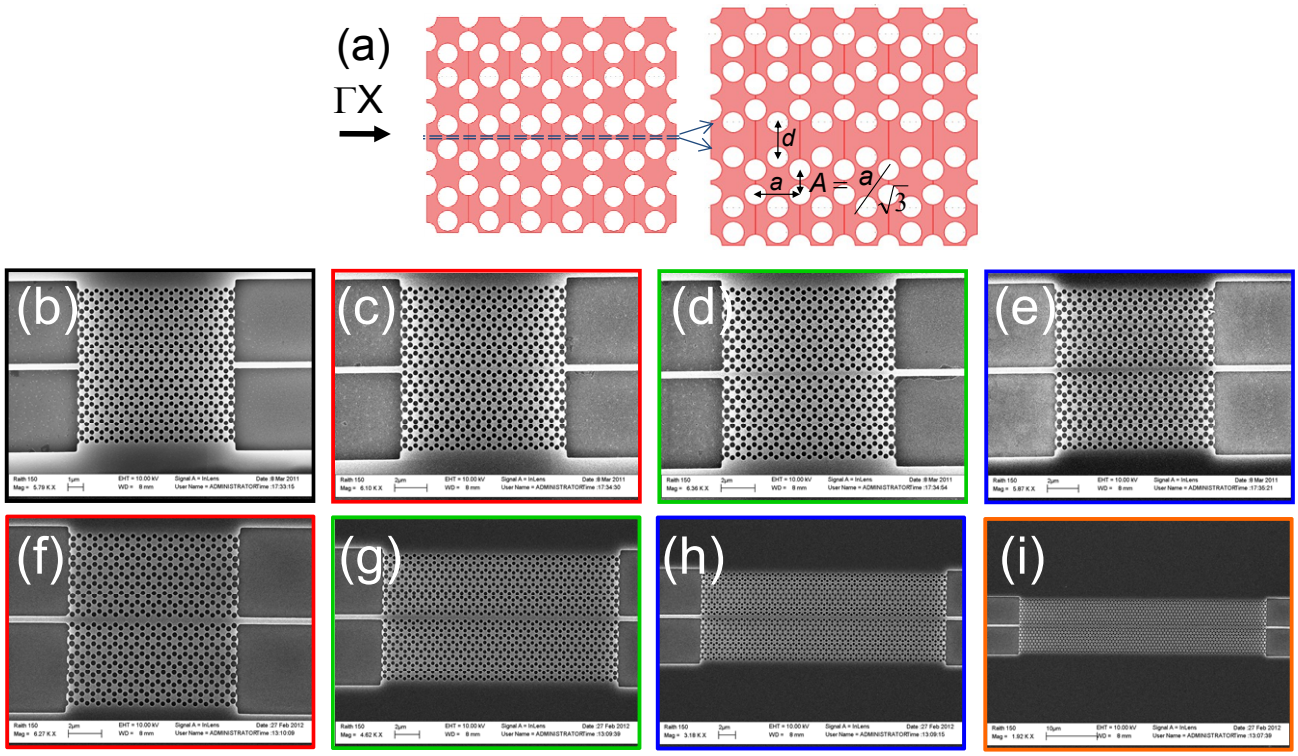

Fig. 4: (Color online) (a) Sketch of the proposed waveguide defect controlled by the parameter d in the honeycomb-lattice (d=A means a perfect structure without waveguide). (b-e) SEM images of the fabricated waveguides with a lattice orientation of 0º degrees: (b) d=A (no waveguide), (c) d=1.2A, (d) d=1.4A and (e) d=1.6A. The total length of these honeycomb waveguides is 10 μm. (f-i) SEM images of the fabricated waveguides with a lattice orientation of 0º degrees and d=1.6A: (f) 10 μm, (g) 20 μm, (h) 30 μm and (i) 50 μm of total length. Input and output waveguides are 400 nm wide which are adiabatically widened to 3-μm width waveguides used as input and output ports for external optical fibers.

Figure 5(a) shows the band structure of a suspended silicon PCS with a honeycomb lattice of holes for different values of d: A, 1.2A, 1.4A and 1.6A. The refractive index of silicon in the simulations has been chosen to be 3.45. In the d=A band structure a photonic bandgap for odd-parity guided modes appears in the interval [0.39, 0.45] in normalized frequency units of $\omega a/2\pi c$. By varying the parameter d, we control the waveguide width and the amount of odd-parity guided modes appearing in the photonic band gap as shown in Fig. 5(a). It can be seen that when d is increased there are photonic bands that drop from the continuum of guided modes above the band gap. The frequency region of such bands that is below the light cone corresponds to truly guided modes inherently lossless, in contrast the guided modes in honeycomb-lattices fabricated in semiconductor heterostructures with small-index contrast in the vertical direction [9]. Interestingly, the guided bands are quite flat so they will display slow-light propagation, which could give rise to enhanced acousto-optical interactions [5].

The measured spectra for TM-polarized light are shown in Fig. 5(b) for different values of d. For d=A, the waveguide width is zero so we have a perfect honeycomb lattice photonic crystal and a high attenuation (~35 dB) in the wavelength region corresponding to the predicted odd band gap is observed. This high attenuation is also observed when the lattice is arranged so that incidence is along the ΓM direction, which confirms the prediction of a two-dimensional photonic bandgap for odd modes. When d is increased, high transmission zones appear in the region inside the calculated odd-parity photonic bandgap. We partly attribute this high-transmittance to the excitation of the guided modes calculated before (see Fig. 5(a)). However, we do not observe discrete modes but a continuous band covering almost the full measured wavelength range. We attribute this to the excitation of leaky modes above the light line (see Fig. 5(a)). Therefore, to fully observe the excitation of the predicted guided modes, longer waveguides are required so that only truly guided modes can reach the PCS waveguide end [10]. The measurements for longer d=1.6A waveguides (see Fig.

4(f-i)) are shown in Figure 5(c). It can be seen that when the length is increased, two narrow transmission bands are kept in the bandgap. These high transmission regions correspond to the two first guided modes within the bandgap. The other two guided modes appearing inside the bandgap for d=1.6A cannot be excited due to symmetry reasons, as it has been proved by simulations (not shown here). A rough estimation of the propagation losses for the two observed bands gives us a value of 100 dB/mm. This is a quite high value that can be explained by two main reasons. First, propagation losses are produced mainly by scattering in the etching-induced roughness at the sidewalls, and this scattering grows with the waveguide thickness, so we can expect higher losses in our waveguides than in typical triangular-lattice photonic crystal waveguides created in 220-nm thick silicon. And second, we are exciting slow-light modes so the propagation losses will grow with the inverse of the group velocity. We are confident in that by improving the fabrication processes, propagation losses of the order of 10dB/mm are under reach, so these waveguides could be used for coupling light with guided acoustic modes.

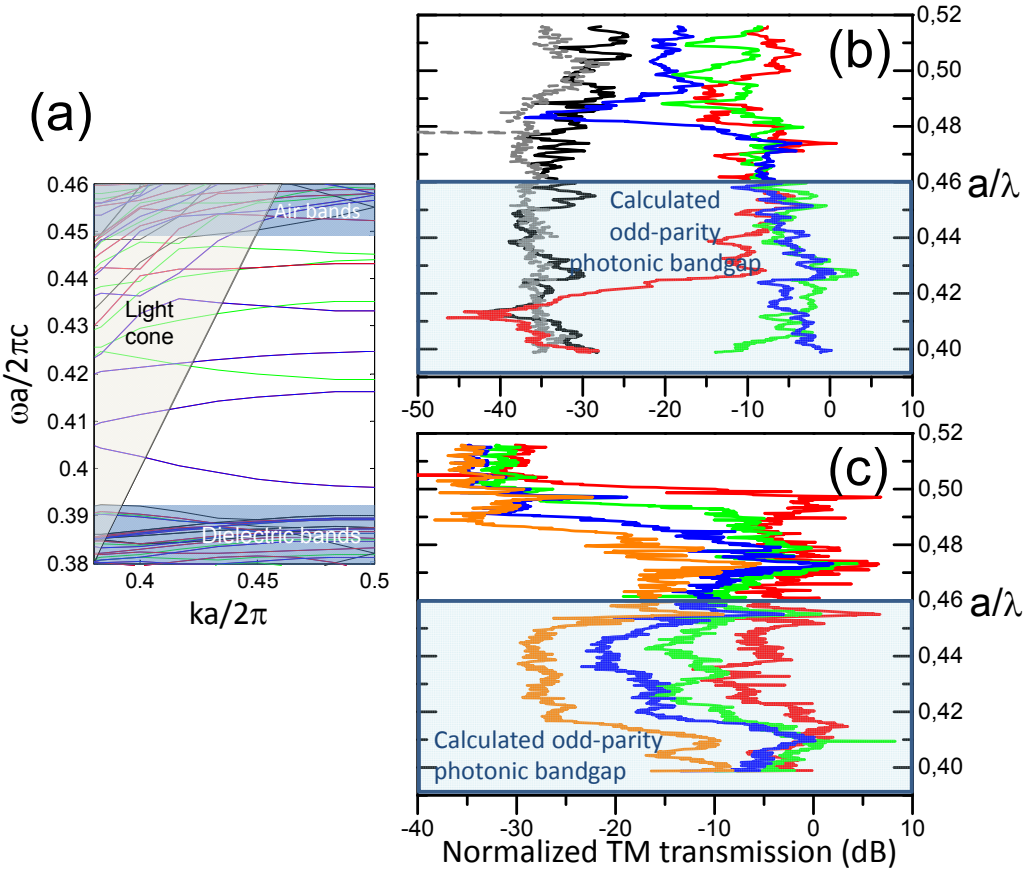

Fig. 5: (Color online) (a) Calculated bands for different values of d: A (black curves), 1.2A (red curves), 1.4A (green curves) and 1.6A (blue curves). (b) Measured normalized spectra for TM-polarized light and for different values of d: A and 45º degree-lattice (gray curve), and with 0º degrees-lattice; A (black curves), 1.2A (red curves), 1.4A (green curves) and 1.6A (blue curves). The total length of these honeycomb waveguides is 10 μm. (c) Measured normalized spectra for TM-polarized light for membranes with 0º degrees-lattice and d = 1.6A for different total length: 10 μm (red curves), 20 μm (green curves), 30 μm (blue curves) and 50 μm (orange curves).

Interestingly, we observe that for the structure without defect the transmission is low even at frequencies over the predicted band gap. This low transmittance can be explained by two different reasons. First, it can happen that the odd modes over the band gap cannot be excited by an optical signal coming from the input silicon waveguide owing to symmetry mismatching. However, it is quite improbable that none of the photonic modes existing in that region is excited. Therefore, we give more credit to the second possible explanation: the excitation of multiple photonic modes in the photonic crystal region. In this case, modes with very different wave-vectors (including modes with high transverse wave vectors as a consequence of the small width of the optical signal coming from the input silicon waveguide) will be

excited and they can also couple slab-modes out of the photonic-crystal region so that an very small amount of power will be finally coupled to the output waveguide. This mechanism also explains why a high transmission is observed out of the band gap region when the line-defects are introduced: the high-index region between the side photonic crystal region inhibits the divergence of the input signal coming from the waveguide and provides a channel for guiding light towards the output waveguide using the mechanism of total-internal reflection as in conventional dielectric waveguides.

3.2 Square Lattice

Square-lattice can also be designed to display a complete photonic bandgap forbidding guided modes for both odd and even symmetries [5]. In this case, the square-lattice structure has been designed to have a wider photonic band gap for even symmetry modes which can be excited using TE polarized light. Figure 6(a) shows the sketch of a square-lattice PCS membrane where *a* is the lattice period, *h* is the slab thickness, *r* is the radius of the holes and *d* is the thickness of the photonic waveguide created by eliminating a hole line along the ΓX direction. The parameters (a = 500 nm, r = 210 nm and h = 325 nm) were chosen so that the structure provides a wide photonic band gap for even-parity modes in the wavelength region around 1550 nm. For instance, a minimum spacing between adjacent holes of 50 nm is considered. Figure 6(b-e) shows SEM images of the fabricated waveguides with a lattice orientation of 0º degrees and *d=0* (b) or *d ≠0* (c), and a lattice orientation of 45º degrees and *d=0* (d) or *d ≠0* (e).

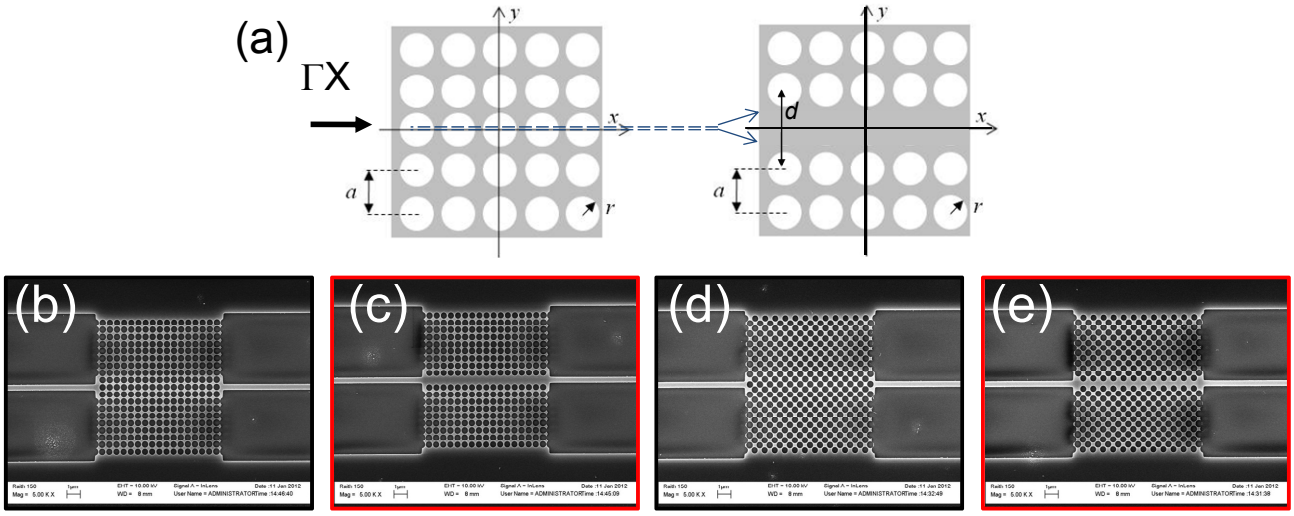

Fig. 6: (Color online) (a) Scheme of the proposed waveguide defect in the square-lattice where the waveguide defect is produced by eliminating a line of hole in the center of the lattice (*d* = 0 means a perfect structure without waveguide). (b-e) SEM images of the fabricated waveguides with: a lattice orientation of 0º degrees and *d=0* (b) or *d ≠0* (c), and a lattice orientation of 45º degrees and *d=0* (d) or *d ≠0* (e). The total length of these honeycomb waveguides is 10 μm. Input and output waveguides are 400 nm wide which are adiabatically widened to 3-μm width waveguides used as input and output ports for external optical fibers.

Figure 7(a) shows the band structure for even-parity (TE-polarized) of a square-lattice PCS (a = 500 nm, r = 210 nm and h = 325 nm) with a lattice orientation of 0º degrees (ΓX direction) and *d ≠0*. The band structure show two photonic bandgaps for guided modes in the intervals [0.32, 0.34] and [0.35, 0.38] in normalized frequency units of $\omega a/2\pi c$. The frequency region of bands that is below the light cone corresponds to truly guided modes inherently lossless. Interestingly, this structure also has a guided band around 0.32 (normalized frequency units) that is quite flat and could also give rise to enhanced acousto-optical interactions [5]. The measured spectra of the square-lattice structure with 0º degrees for TE-polarized light are shown in Fig. 7(b). For a perfect square-lattice photonic crystal (*d=0*, black curve) a high attenuation (~30 dB) is observed. This high attenuation is also observed in the transmission spectra (black curve, Fig. 7(c)) of a perfect 45º degrees square-lattice PCS (ΓM direction). This optic transmission behavior of the structures without defect can be explained with the same reasons given in the last paragraph of the honeycomb point (see 3.1).

The transmission spectra of the 0º degrees square-lattice PCS with *d ≠0* (Fig. 7(b), blue curve) show a depth gap (~30 dB) in the region [0.36, 0.37] inside the calculated even-parity photonic bandgap [0.35, 0.38]. The high transmission in the others normalized frequency zones can be partly attributed to the excitation of the guided modes calculated before

(see Fig. 7(a)), whereas the small drop around 0.32 and the following increase in the transmission at 0.31 can be attributed to the calculated even-parity bandgap between [0.32, 0.34] and to the flat guided mode around 0.32, respectively. A change in the square-lattice PCS parameters (*a, h* and *r*) induce a shift in the transmission spectra. So, in the transmission spectra (Fig. 7(b)) of the square-lattice PCS with a parameters of a = 500 nm and r = 230 nm (green curve), and a = 500 nm and r = 210 nm (red curve) a shift of the depth gap [0.36, 0.37] toward high normalized frequencies is observed. This frequency shift is due to the hole radius change.

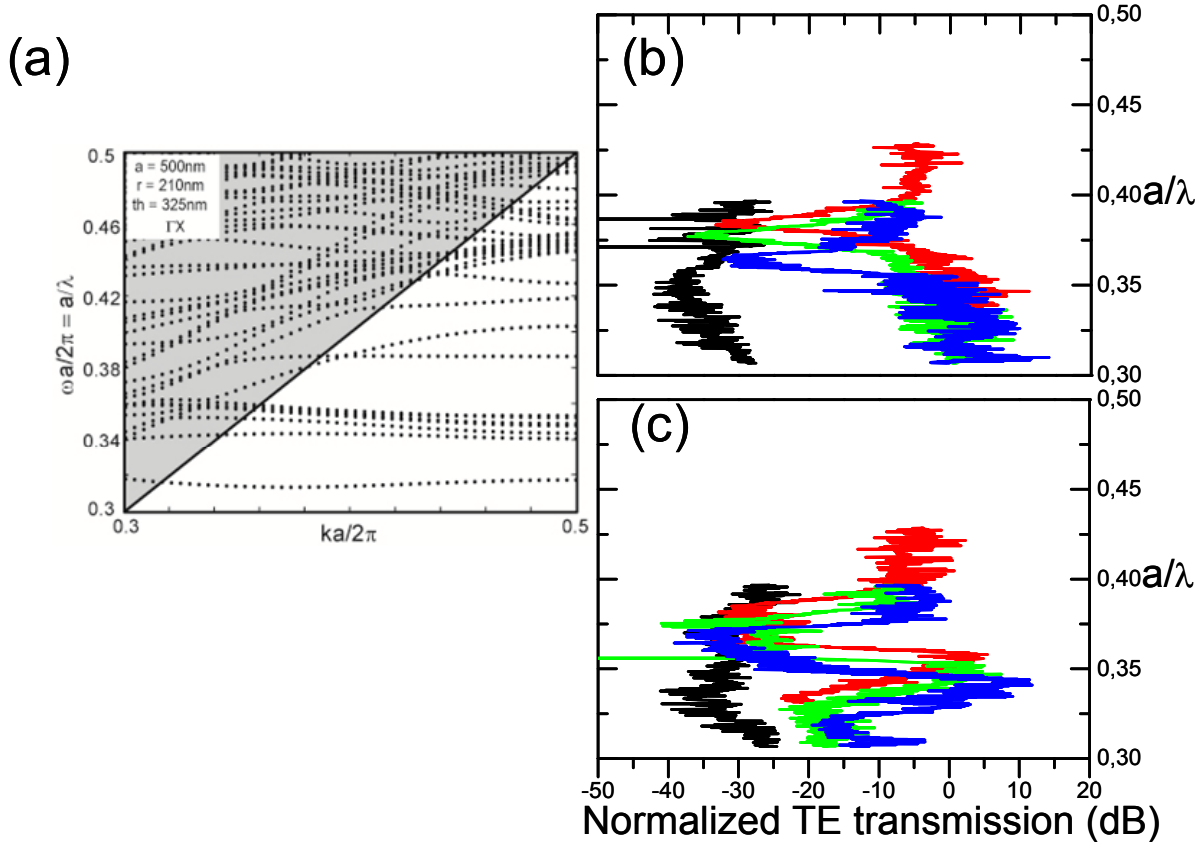

Fig. 7: (Color online) (a) Calculated bands for a square-lattice photonic crystal with a waveguide defect (*d*), a period of a = 500 nm, a hole radios of r = 210 nm, a thickness of h = 325 nm, and lattice orientation of 0º degrees. (b) Measured normalized spectra for TE-polarized light for membranes with 0º degrees-lattice, a waveguide defect (*d*) and a period and hole radios of: a = 540 nm and r = 250 nm (red curve), a = 500 nm and r = 230 nm (green curves), 500 nm and r = 210 nm (d =0, black curves), and a = 500 nm and r = 210 nm (blue curves). (c) Measured normalized spectra for TE-polarized light for membranes with 45º degrees-lattice, a waveguide defect (*d*) and a period and hole radios of: a = 540 nm and r = 250 nm (red curve), a = 500 nm and r = 230 nm (green curves), 500 nm and r = 210 nm (d =0, black curves), and a = 500 nm and r = 210 nm (blue curves). The total length of these membranes is 10 μm.

The transmission spectra measurements of the 45º degrees square-lattice PCS with $d \neq 0$ (see Fig. 6(e)) are shown in Figure 7(c). The measure spectra of the square-lattice with a = 500 nm and r = 210 nm (blue curves) show two gaps, one of them in the region [0.35, 0.38] with a depth ~30 dB and a second in the interval [0.31, 0.33] of ~18 dB. This second gap is finished by a sharp transmission increase around 0.31, which agrees with the flat guide mode observed in the photonics bands simulations along ΓM direction (not shown here for simplicity). Such as can be seen in the curves green (a = 500 nm and r = 230 nm) and red (a = 500 nm and r = 210 nm), the change of the hole radius also induce a shift in the transmission spectra for the 45º degrees square-lattice. So, the deep transmission dip in the interval [0.35, 0.38] is shifted toward high normalized frequencies, together with the rest of the spectra.

4. CONCLUSIONS

In summary, we have demonstrated experimentally the guiding of light in the 1550 nm wavelength region along line-defect created in suspended silicon photonic crystal with a honeycomb and square lattice of holes. Our calculations show that the guided modes are below the light line so they are lossless in theory. Since the studied photonic crystal structure also displays a band gap for GHz acoustic waves, it can be a proper two-dimensional platform for simultaneous guiding and enhanced interaction of light and sound as well as to observe novel optical and optomechanical effects.

ACKNOWLEDGEMENTS

This research has received funding from the European Community's Seventh Framework Programme (FP7/2007-2013) under grant agreement number 233883 (TAILPHOX). D.P. acknowledges their grant of the Spanish Ministry of Science and Education under JCI-2010-07479.

REFERENCES

[1] Mekis, A., Chen, J. C., Kurland, I., Fan, S., Villeneuve, P. R. and Joannopoulos, J. D., "High transmission through sharp bends in photonic crystal waveguides," Phys. Rev. Lett. 77, 3787-3790 (1996)

[2] Notomi, M., Yamada, K., Shinya, A., Takahashi, J., Takahashi, C. and Yokohama, I., "Extremely large group-velocity dispersion of line-defect waveguides in photonic crystal slabs," Phys. Rev. Lett. 87 (25), 253902 (2001)

[3] Joannopoulos, J. and Winn, J., [Photonic Crystals: Molding the Flow of Light], Princeton Univ. Press, (2008)

[4] Pennec, Y., Djafari Rouhani, B., El Boudouti, E. H., Li, C., El Hassouani, Y., Vasseur, J. O., Papanikolaou, N., Benchabane, S., Laude, V. and Martinez, A., "Simultaneous existence of phononic and photonic band gaps in periodic crystal slabs," Opt. Express **18**, 14301-14310 (2010)

[5] Laude, V., Beugnot, J. C., Benchabane, S., Pennec, Y., Djafari-Rouhani, B., Papanikolaou, N., Escalante, J. M. and Martinez, A., "Simultaneous guidance of slow photons and slow acoustic phonons in silicon phoxonic crystal slabs," Opt. Express 19, 9690-9698 (2011)

[6] Maldovan, M. and Thomas, E., "Simultaneous localization of photons and phonons in twodimensional periodic structures", Appl. Phys. Lett. 88, 251907 (2006)

[7] Eichenfield, M., Camacho, R., Chan, J., Vahala, K. J. and Painter, O., "A picogram- and nanometre-scale photonic-crystal optomechanical cavity," Nature 459 (7246), 550–556 (2009)

[8] Eichenfield, M., Chan, J., Camacho, R., Vahala, K. J. and Painter, O., "Optomechanical crystals," Nature 462 (7269), 78–82 (2009).

[9] Ma, P., Kaspar, P., Fedoryshyn, Y., Strasser, P. and Jäckel, H., "InP-based planar photonic crystal waveguide in honeycomb lattice geometry for TM-polarized light," Opt. Lett. **34**, 1558-1560 (2009)

[10] McNab, S. J, Moll, N. and Vlasov, Y. A., "Ultra-low loss photonic integrated circuit with membrane-type photonic crystal waveguide" Opt. Express 11 (22), 2927-2939 (2003)